Supplementary Information

GPC analysis was performed using tetrahydrofuran as the eluent with a flow rate of 1 mL/min through three PSS SDV columns from Waters Corp (500 Å, 50 Å, and Linear M), each 300 mm long and 8 mm in diameter. A Waters 410 Refractive Index detector was used to monitor elution and analysis was performed using PSS-Win GPC software from Polymer Standards Service. A calibration curve was created using polyisoprene standards from Polymer Standards Service which had molecular weights of 1.08, 3.92, 8.05, 10.9, 15.1, 22.7, 34.3, 56.0, 84.7, 109, 293, 454 and 766 kg/mol.

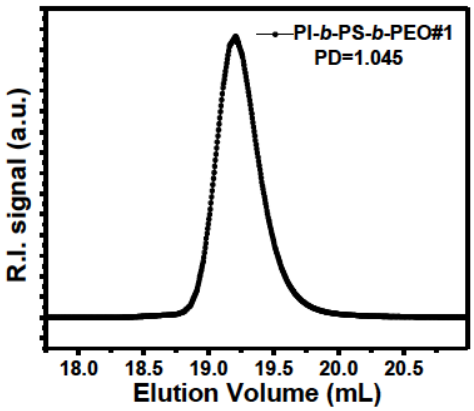

Figure S1. Gel permeation chromatogram for ISO1.

NMR analysis was used to determine the I, S, and O mol fractions from peaks a, b, c, and d (Figure S2). Additionally the I-block microstructure was determined to be 93.3% 1,4-polyisoprene and 6.7% 3,4-isoprene by comparing peaks b and c. Such predominance of 1,4-polyisoprene is typical for anionic polymerization of isoprene in non-polar solvents with lithium cations.

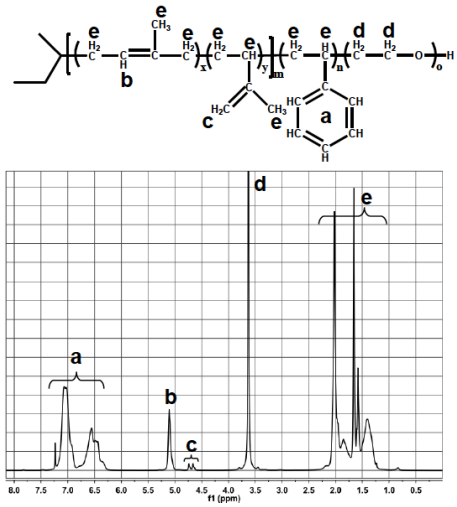

Figure S2. ^{1}H nuclear magnetic resonance spectrum for ISO1 (bottom) indexed according to the contributing protons (top).

Similar SAXS patterns were gathered from different regions of an ISO1 film (Figure S3). The variations in peak intensities as well as the appearance of a shoulder near $(q/q^*_{100})^2=4$ in curve c indicate a strong dependence on sample orientation or perhaps structural heterogeneity in the pure polymer film.

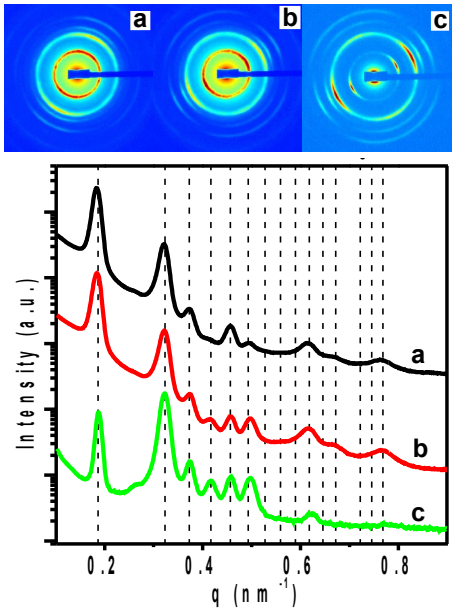

Figure S3. Both 2D (top) and integrated 1D (bottom) SAXS patterns are shown for different regions (a, b, and c) of an ISO1 cast film. Dashed lines indicate the allowed reflections for the $I4_132$ space group of the alternating gyroid which were fit to curve b. The color scale corresponds to the log of the x-ray intensity. The 1D SAXS patterns were shifted vertically for easier viewing. Scattering pattern b was duplicated from Figure 2c for comparison.

Full 2D SAXS patterns are presented for all three nanocomposites (Figure S4 a-c). Samples which have a preferred orientation of grains exhibit variations in the scattering as a function of azimuthal angle. Examples of such variations with azimuthal angle are presented as 1D integrals over narrow angular ranges (Figure S4 d-f).

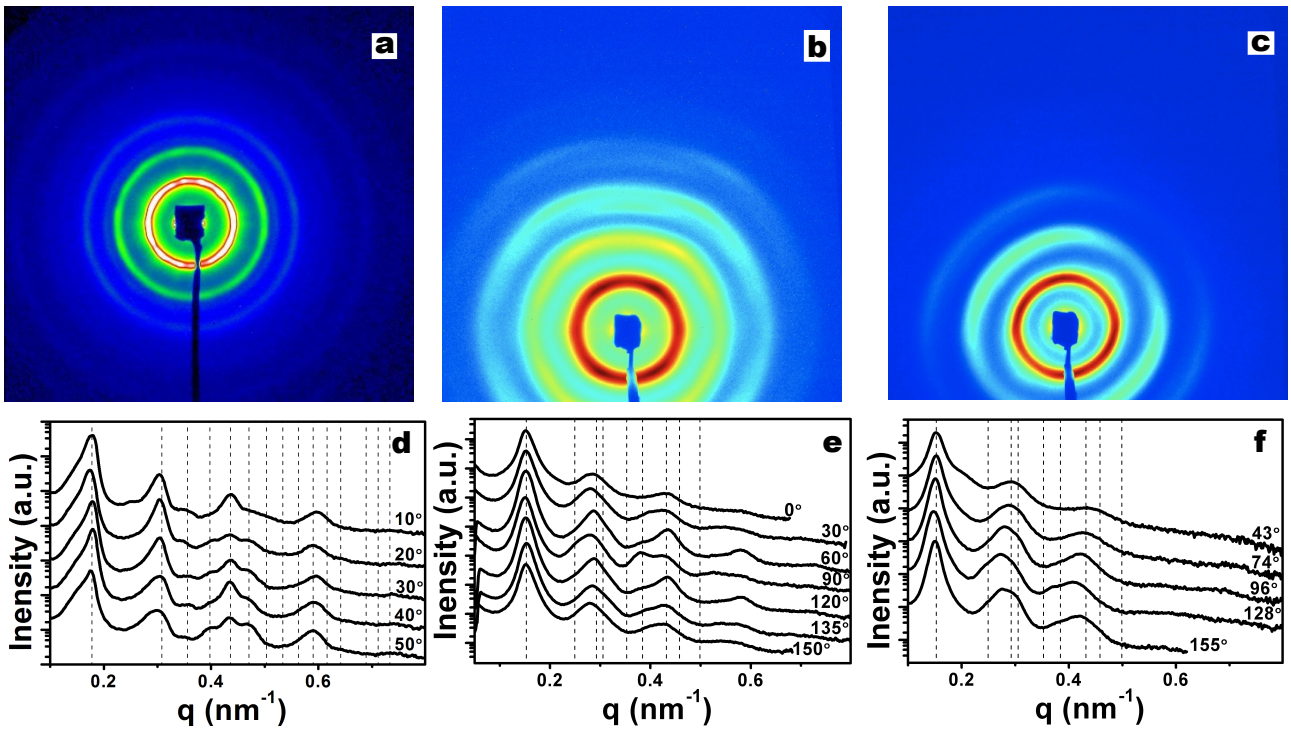

Figure S4. Full 2D SAXS patterns for samples ISO1-N1 (a), -N2 (b), and -N3 (c) are shown with log scale color. Several 1D integrals were shown for each sample at the indicated azimuthal angles ±5°. The 1D patterns in d, e, and f, correspond to samples ISO1-N1, -N2, and -N3. The allowed reflections for either $I4_132$ (d) or Fddd (e,f) space group were indicated with dashed lines. The SAXS patterns in (a) and in (f) at 128° were duplicated from Figure 3 for comparison.

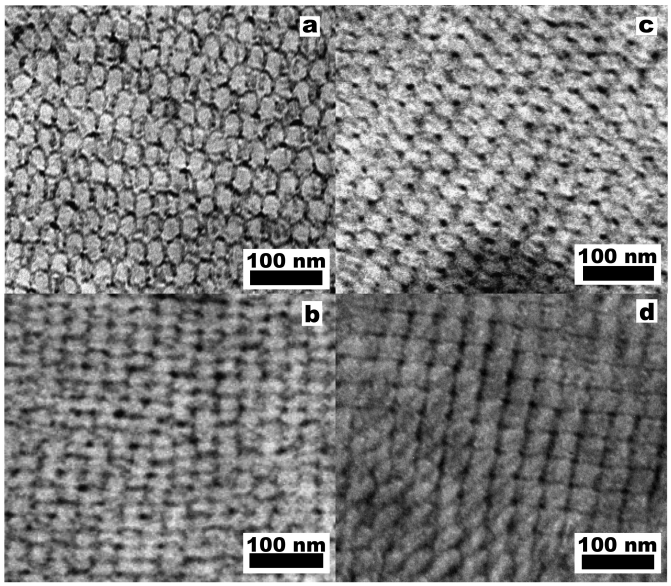

Figure S5. Bright field TEM images of samples ISO1-N1 (a,b) and ISO1-N2 (c,d). Image (a) was duplicated from manuscript Figure 4 for comparison.

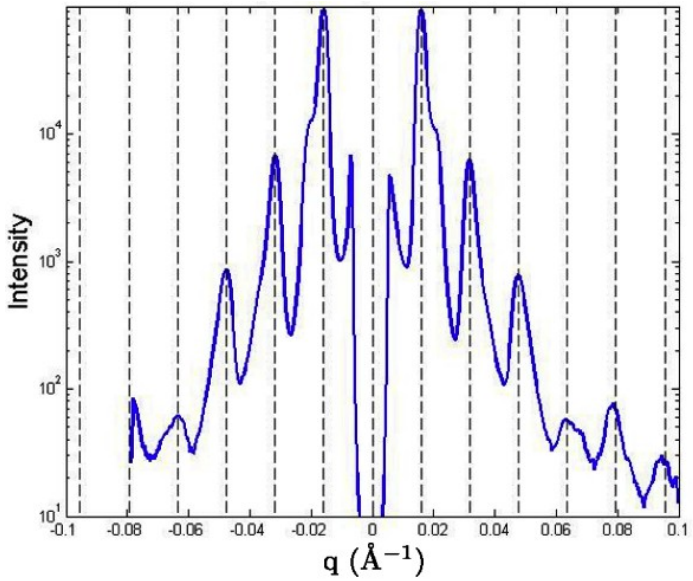

Figure S6. An azimuthally integrated slice from Figure 3A (Φ=90°) showing that along this slice the scattering pattern predominantly corresponds to a lamellar morphology (allowed reflections indicated with dashed lines).

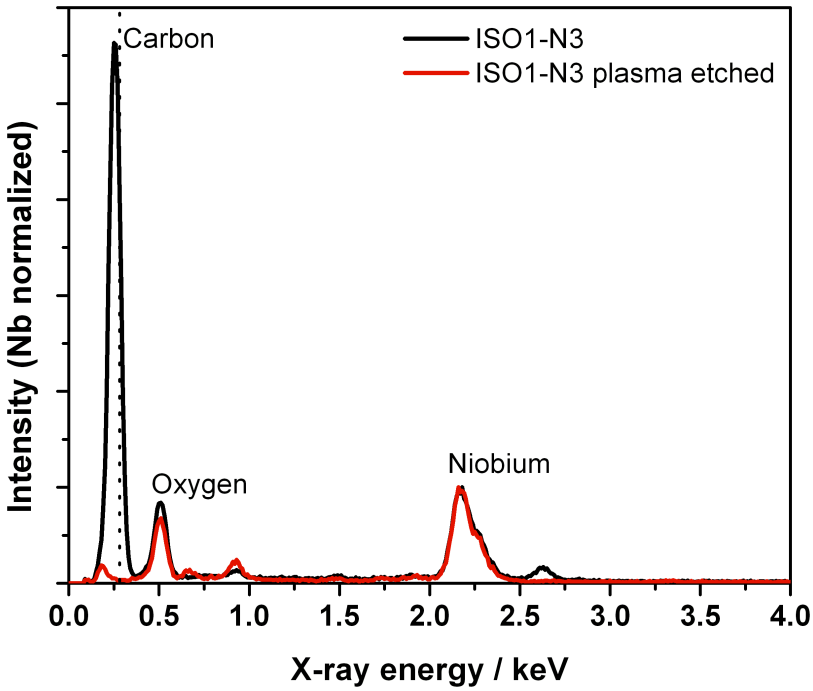

Figure S7. Engery dispersive x-ray spectra of sample ISO1-N3 before and after plasma removal of the polymer. The loss of the carbon peak indicates complete removal of the block copolymer.

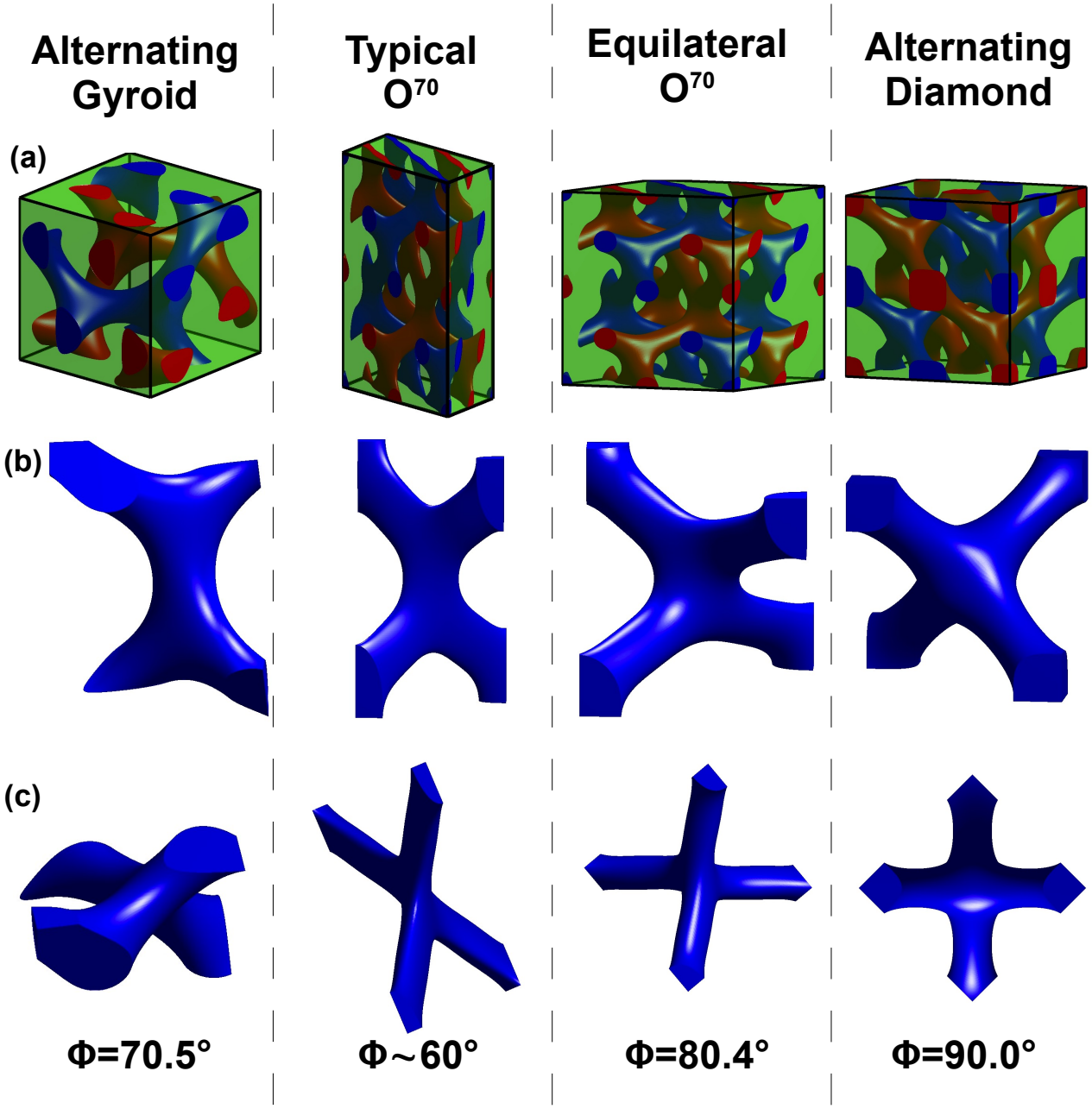

Figure S8. Schematic depicting the geometrical relations between the alternating gyroid, the O^{70}, the equilateral O^{70}, and the alternating diamond. A single unit cell is displayed for each morphology in the first row (a). A subvolume depicting two 3-valent connectors or one 4-valent connector (D^A) are compared for each morphology in the second row (b). Please note the significant compression in the equilateral O^{70} along the z-axis where the two depicted 3-valent nodes are in close proximity. The top views of these same subvolumes (c) are shown for comparison of the projected angles between connectors.